Polymer Bulletin (2022) 79:2383–2409
https://doi.org/10.1007/s00289-021-03623-y

ORIGINAL PAPER

A study on the physical, mechanical, thermal properties and soil biodegradation of HDPE blended with PBS/HDPE-g-MA

E. El-Rafey[1] · Walaa M. Walid[1] · Eslam Syala[1] · Abbas Anwar Ezzat[2] · Salah F. Abdellah Ali[1,3]

Received: 27 August 2020 / Revised: 26 January 2021 / Accepted: 24 February 2021 /
Published online: 12 March 2021

Abstract

In this study, blends of high-density polyethylene/poly(butylene succinate)/high-density polyethylene-grafted maleic anhydride (HDPE/PBS /HDPE-g-MA) blends were prepared by using the injection molding technique. The aftereffect of mixing HDPE-g-MA (as a blend, not as a compatibilizer) and PBS by the different ratios (1, 2, 4 wt%) was investigated by various characterization techniques to give a comprehensive perception of the as-prepared system. The structure was characterized through the FTIR spectra to confirm the existence of PBS and HDPE-g-MA separately in the matrix for each blend that ensures the physical interaction between the components. The mechanical property analysis established that the different ratios of PBS and HDPE-g-MA to the HDPE matrix resembled those of the neat HDPE; however, the elongation at break, the impact strength and hardness of the mixtures were increased by increasing PBS and HDPE-g-MA, respectively. The thermal analysis exposed that the inclusion of PBS caused a decrease in the crystallinity percentage and prompted a decrease in the Melt Flow Index (MFI). The oxidative induction time (OIT) of the neat HDPE had a fluctuating behavior by adding HDPE-g-MA and PBS. The water absorption percentage of the blends was insignificantly increased compared to neat HDPE. The enhanced biodegradation of the blends compared to HDPE could be elucidated by the initiation of microbial deterioration of PBS, inside the HDPE matrix, by the activity of microorganisms that presented in the soil.

✉ Eslam Syala
Eslam.Syala@alexu.edu.eg

[1] Department of Material Science, Institute of Graduate Studies and Researches, Alexandria University, 163 Horreya Avenue, Shatby 21526, Alexandria, Egypt

[2] Petrochemicals Engineering Department, Faculty of Engineering, Pharos University, Alexandria 21311, Egypt

[3] Chemistry Department, College of Science and Arts, Al-Jouf University, Sakaka 2014, Saudi Arabia

Graphical abstract

The mixing of PBS and HDPE-g-MA with HDPE (Fig. a) in different ratios increased the biodegradation of the blends as in Fig. b, c and d. (The pores resulted from degradation are marked in each picture)

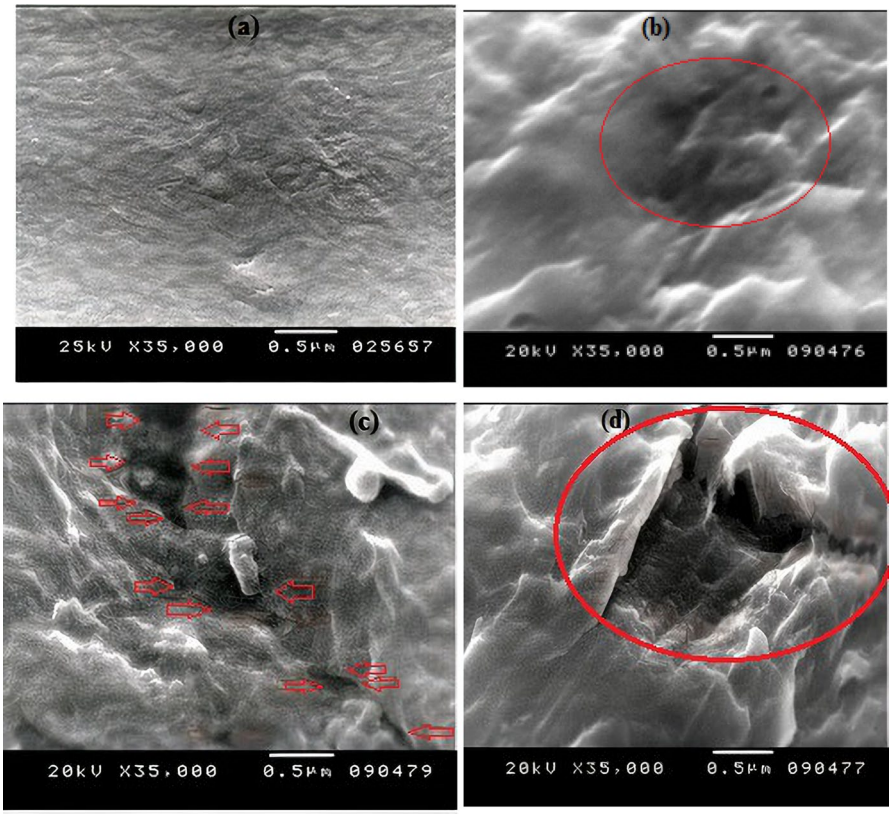

Keywords High-density polyethylene · Poly(butylene succinate) · Thermal properties · Biodegradation

Introduction

There are worldwide research attempts to progress biodegradable plastics as a waste administration solution for polymers in the ecosystem [1]. Biodegradable polymers present a potential solution to waste disposal issues associated with conventional petroleum-derived plastics. The first introduction of biodegradable polymers was in the 1970s in the molded articles, sheets, films, etc. [2]. Biodegradation is the biotic degradation of materials by the activity of microorganisms just like bacteria, fungi and algae. Biodegradation is also predicted to be the essential mechanism of

discarding of most chemicals freed into the environment. This process points to the degradation of polymers by the act of living microorganisms to generate degraded products [3].

Compared to today's synthetic polymers, biopolymers can potentially offer higher biodegradability, better recyclability and lower process energy requirements with a smaller environmental footprint overall [4].

A degradable polymer is a polymer that undergoes a considerable variation in the chemical structure under particular environmental conditions and by the participation of microorganisms.

Synthetic polymers represent the dominant surface of waste dumps [5]. The solution to this problem may be the synthesis and use of biodegradable polymers. Biodegradable polymers can be categorized into four classes: (1) the mixtures of artificial polymers and substances that are easy to digest by microorganisms, (2) synthetic polymers with groups that are susceptible to hydrolytic microbial attack (e.g., polycaprolactone), (3) the biodegradable synthetically polymers that need chemical environments (like a human body that contains glutathione and that are used to destroy the coating of a drug to accomplish a better delivery) and (4) the biopolyesters from bacterial sources. The most prevalent and important biodegradable polymers are aliphatic polyesters (e.g., polylactic, poly(ε-caprolactone), poly(3-hydroxybutyrate) and polyglycolic acid) [6]. Their decomposition will aid in increasing the durability of landfills by lowering the mass of garbage; they could be recycled to useful monomers and oligomers by microbial and enzymatic handling [7].

The fabrication of plastic blends is very important for reasons concerning improving the properties and processing of plastic, decreasing the environmental effects and reducing the cost [8]. These blends can be attained by mixing nonbiodegradable and biodegradable polymers. Polyethylene (PE) is one of the largest widespread polyolefins derived from oils. It can be considered the most essential thermoplastic polyolefin; it makes up approximately 64% of all produced polymers [9]. PE does not dissolve in any solvent at room temperature, whereas it dissolves smoothly in aromatic and chlorinated hydrocarbons that have a higher melting point compared to PE. Upon cooling, these solutions incline to form gel [10]. Besides, PE does not degrade after use; so, it must be disposed off [11].

HDPE is a white opaque material that is the nearest in structure to raw PE. It consists mainly of unbranched molecules with very little defects that may damage its linearity. It has a high degree of crystallinity [12]. Its resins most often have densities in the bounds of 0.94–0.97 g/cm^3. Moreover, HDPE has acceptable mechanical strength with relatively hard and high impact properties; it is chemically inert and very resistant to chemicals and corrosion and capable to bear high temperatures up to 120 °C without varying its properties [13]. HDPE is easy to compound with several additives to promote its properties that can be tailored in line with the desired applications [14].

Commercially manufactured biodegradable polyesters, just like poly(lactic acid) (PLA), poly(3-caprolactone) (PCL) and poly(b-hydroxybutyrate) (PHB), are the most conventional and profoundly studied. However, these biodegradable polymers have some drawbacks that limit their end use, such as low heat resistance, high production cost and inferior mechanical properties [11, 15]. Poly(butylene succinate)

(PBS) is an emerging biodegradable and biomass polyester that can be synthesized by the condensation of succinic acid and 1,4-butanediol [11]. PBS has desirable melt processability and superior mechanical characteristics on a level with those of the extensively used PE and polypropylene [16]. It is semicrystalline polyester; its mechanical properties, flexibility, transparency and biodegradability are established on the structures and the crystallinity degree. The crystallization attitude of PBS resembles that of PE. It has a melting peak close to 112–116 °C. Its thermogravimetric analysis curve reveals that it shows weight losses of 5, 50 and 90% at 325, 400 and 424 °C, respectively, in air or nitrogen. On the contrary, PBS shows thermal deterioration when extruded at 200 °C [17]. It possesses satisfactory tensile and impact strengths, moderate rigidity and hardness, plus being a typical tough polymer. It can find applications in agriculture, medicine, construction, fishery, packaging, etc. [18].

HDPE is a nonpolar polymer, but PBS is a polar polymer; therefore, the mix of HDPE and PBS is an immiscible blend that has poor physical properties ascribable to the weak interfacial adhesion among them [14]. Wherefore, attempts focused on using the maleic anhydride-grafted PE (PE-g-MA) as a blend to optimize the interfacial tension between PE and PBS were performed. For that reason, the selection of the components of the existing blend was based on these criteria.

It has been stated that some copolymers or graft polymers that possess reactive groups can reduce the volume of the disseminated phases and enhance the interfacial bonding [19]. HDPE-g-MA can improve the dispersion and adhesion abilities between polymers phases, metals, glasses and ceramics [20].

Darshan et al. [11] prepared PBS/HDPE blends and added HDPE-g-MA and carbon nanotubes (CNT) as compatibilizers and nanofillers, respectively. HDPE-g-MA increased the crystallization temperature of PBS and hence the thermal constancy of the blend. The involvement of HDPE-g-MA and CNT improved also the rheological features of the blend.

Huang et al. [21] studied the degradation conduct of the blend (PBS/PCL) in the local soil culture solution. The results stated that the composite's original functional groups were retained even after the blending of PBS and PCL and the forming of hydrogen bonds. In the compost culture solution, the composite based on PBS and PCL degraded well. This composite's weight and weight loss were decreased by 32.67 and 8.76%, respectively, after 60 days. PCL degraded more rapidly than PBS, while the mixture of PBS and PCL degraded even more quickly.

Yang et al. [22] observed the shear and extension properties of HDPE and PBS mixtures using capillary rheometers to explore the repercussion of the processing circumstances and the mixing ratios on the flow demeanor and the predictive capabilities of the extension master curve. They proved that the blend's shear flow obeyed the power law and the influence of PBS content on shear-thinning behavior was evident. The viscosity of the mixtures was reduced with the extensional strain rate and the increase in the PBS bulk.

Ajcharaporn Aontee and Wimonlak Sutapun [23] studied the influence of HDPE-g-MA on both the thermal and mechanical properties and also the crystallinity percentage (χ_c %) of HDPE/PBS/HDPE-g-MA blends. The blends were prepared at a PBS/HDPE weight ratio of 30/70, and the HDPE-g-MA was used at

contents of 2, 4, 6 and 8 parts per hundred of PBS and HDPE. The results demonstrated that the stress at break and yield strength of HDPE/PBS/HDPE-g-MA blends insignificantly increased with the insertion of HDPE-g-MA more than 2 PPH. Further incorporation of HDPE-g-MA to the two blends led to higher elongation at break and increasing the impact strength, while Young's modulus of blends exhibited an insignificant variation.

In the present study, the HDPE was blended with several proportions of PBS and HDPE-g-MA. The influence of increasing both PBS and HDPE-g-MA contents on the mechanical, thermal and physical properties, the degree of crystallinity and the biodegradation of HDPE was investigated and discussed. The novel in this study (than the previous) is performing many characterization techniques to give a comprehensive image of the studied system.

Methodology

Sample preparation

Powder properties

Virgin pure powder of HDPE grade (HDPE 6070) was directly gained from the polymerization reactor in Sidi Kerir Petrochemical Company (SIDPEC), Alexandria, Egypt. An injection molding grade of HDPE 6070 powder was used (which does not contain any additives like commercial HDPE 6070 pellets). Poly(1, 4-butylene succinate) (PBS) was supplied from Sigma-Aldrich Co. Ltd., UK. It was white pellets with a MFI of 10 g/10 min (2.16 kg and at 190 °C), a density of 1.3 g/ml at 25 °C and a melting temperature of 120 °C. Also, HDPE-g-MA was supplied from Sigma-Aldrich Co. Ltd., UK. It was in the shape of off-white pellets with a melting temperature ≈ 140 °C and 515 cps viscosity.

Preparation of HDPE/PBS/HDPE-g-MA blends

The powder was mixed firstly in a robot coupe mixer for 6 min at speed of 3000 rpm (to achieve homogeneity and good distribution and to gain stabilized morphology) and dried then by a vacuum oven at 50 °C for 24 h earlier to the preparation to avoid trapped bubbles during molding. The injection molding of the specimens was performed via an injection molding machine-type (Arburg all Rounder420C-Golden Edition, Germany) single screw. The processing conditions of the machine were temperature profile feeder: T1:210 °C, T2:220 °C, T3:220 °C, T4:220 °C and T5:215 °C, screw speed: 90 cm/sec, injection press: 1200 bar, cooling time: 60 s and mold temperature: 45 °C. The blends were mixed and named corresponding to the compositions in Table 1.

Table 1 Chemical composition of the synthesized blends

Sample code	HDPE (wt%)	PBS (wt%)	HDPE-g-MA (wt%)
S0	100	0	0
S11	98	1	1
S12	97	1	2
S14	95	1	4
S21	97	2	1
S22	96	2	2
S24	94	2	4
S41	95	4	1
S42	94	4	2
S44	92	4	4

Structural analysis (Fourier transform infrared analysis (FTIR))

The structural examination of the prepared composites was obtained via recording infrared spectra by using (Spectrum Two FTIR spectrometer—PerkinElmer). Pieces of the samples were ground to powder form and alloyed with KBr to form pellets. The test was accomplished at room temperature in the wavelength range of 450–4000 cm^{-1} with a resolution of 1 cm^{-1}.

Thermal characteristics

The melting temperature (T_m) and the heat of fusion (ΔH) were obtained via differential scanning calorimetry (DSC), Q1000 TA-Instrument PerkinElmer according to ASTM D3418-15 [24]. 8 mg of the samples was kept in aluminum capsules and heated from 40 to 200 °C with a heating rate of 5 °C/min.

The mechanical properties

Tensile strength and elongation at break

The tensile properties of the prepared composites were evaluated by the universal testing machine with load cell 5 KN (Zwick /z005, Germany). The dumbbell-shaped specimens were formed and tested at room temperature. The samples were familiarized before performing the test at the laboratory conditions for 24 h. The tensile test was executed in uniaxial tension at a crosshead speed of 20 mm/min in accordance with ASTM D638-14 [25].

Impact test

This test was performed by using the resil impactor test machine (CEAST, Italy) in conformity with ASTM D 4812–19 [26]. The energy released from standardized pendulum-type hammers with one pendulum swing is the magnitude of the impact (60). All specimens were conditioned before testing at the laboratory conditions for 24 h and tested at room temperature and relative humidity 23 ± 2 °C and 50 ± 5%, respectively. Five samples were fitted carefully to the test to shock with hammer load 7.5 J.

Hardness test

As for the present series, the durometer hardness test was implemented at room temperature in keeping with ASTM D2240-15 using Ray-Ran STD227 durometer hardness tester (shore *D*) [27]. Values gained from the hardness test are arbitrary and there are no absolute standards of hardness [28].

Morphology studying

Scanning electron microscopy (SEM; JEOL, Japan JSM-5300) was employed to examine the surface morphology of the HDPE, PBS and HDPE-g-MA samples at an accelerated voltage of 25 kV. The fractured surfaces of the specimens were coated with a thin overlay of gold–palladium to prevent electrical discharge. The test was executed in the central laboratory, Faculty of Science, Alexandria University.

Physical properties

Melt Flow Index (MFI)

MFI of HDPE and all blends were measured in a Ceast plastometer following ASTM D1238–13 [29].

Water absorption test

The test is used to detect the quantity of water absorbed and it was performed according to ASTM D570–98 [30]. Samples were sunk in distilled water and preserved at room temperature for 9 weeks. During this time, they were taken from the water at 1-week intervals, gently wiped by tissue paper to eliminate excess water from the surface and immediately weighed using an electronic digital balance to detect the percentage of water uptake according to:

$$\text{Water Absorption } \% = \frac{\left(M_t - M_0\right)}{M_0} \times 100$$

where M_0 and M_t represent the dry initial weight and the weight after dipping in water, respectively.

Oxidative induction time (OIT)

OIT of HDPE/PBS/HDPE-g-MA composites is a qualitative assessment of the degree of oxidative stabilization and it can be determined through employing differential scanning calorimetry (Netzsch DSC214, Germany). The samples and reference material were heated at an unvarying rate in an inert gaseous ambiance (Nitrogen). When a definite temperature was achieved, the ambiance was converted to oxygen and held at an identical flow rate. The specimens were then retained at an invariable temperature up till the oxidative reaction was noted in the thermal curve. The analysis temperature that was used in this test was set at 200 °C. The test was executed in keeping with the ASTM D3895–07 [31]. The test has proceeded at the Polyethylene laboratory of Sidi Kerir Petrochemical Company (SIDPEC), Alexandria, Egypt.

Biodegradation test

The biodegradability of the samples was examined by the soil interment degradation method which was performed in a plastic box by using wet soil that was extracted from El-Mahmoudia canal, Alexandria, Egypt. To assure enough moisture content, the samples were moistened every two days. The temperature and humidity of the soil were also adapted every two days. The plastic box was divided into five sections, each section contained five specimens; one per sample, only one section was dug out every month to examine the samples contained, and then, all the contained specimens were stayed out from the test. The specimens were sliced into square shape 1 cm × 1 cm and a thickness of 5 mm, dried in a vacuum oven at 50 °C, weighed and then buried in the prepared soil mud. The mud soil contained various groups of Bacillus bacteria of the genus (*Bacillus spp*) such as *Bacillus coagulans*, *Bacillus and Xanthomonas.* Other bacteria belonging to the genus (*Corynebacterium spp*) fungi such as *Fusarium solani*, *Fusarium oxysporum* and *Rhizoctonia solani* with a pH of 7.41 as listed in the report issued by the faculty of Agriculture, Alexandria University, Egypt. The temperature was set at room temperature (25 ± 2 °C) with a minimal air flow rate. Each specimen was removed, laundered with distilled water and dried up in a vacuum oven at 50 °C for 24 h and weighed to record the weight loss percentage. Weight loss percentage was calculated relating to the next equation.

Weight loss $\% = \frac{(W_i - W_f)}{W_i}$ [21] where W_i and W_f are the weights before and after soil burial, respectively. The test was performed according to ASTM D5988–18 [32].

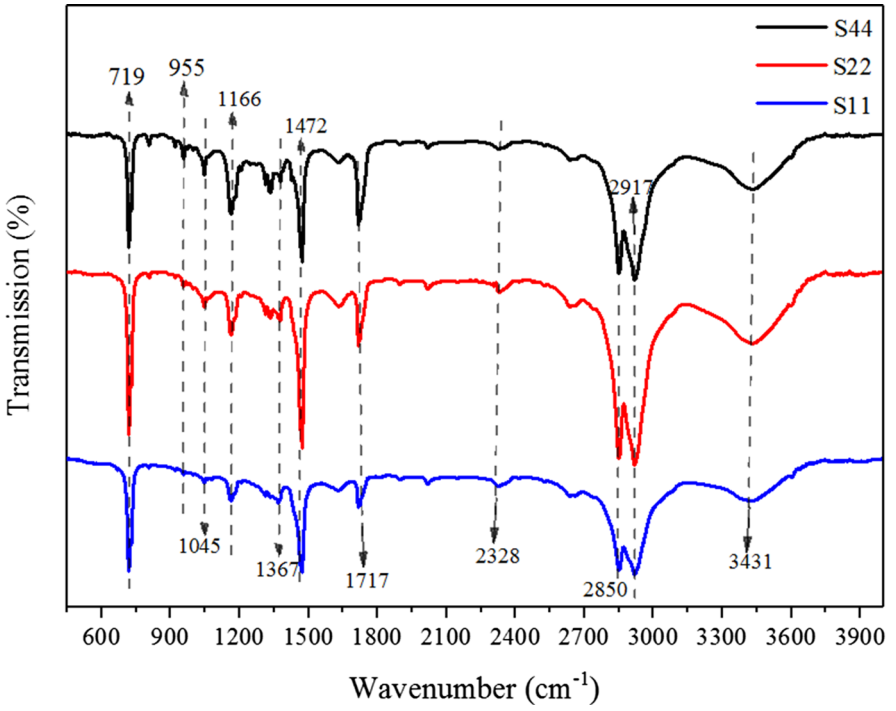

Fig. 1 FTIR Spectra of S11, S22 and S44 blends as representatives to the prepared series

Results and discussion

Structural analysis (FTIR)

Figure 1 and Table 2 show the FTIR peaks assignments of the different ratios of HDPE, PBS and HDPE-g-MA blends. The distinct assignments were around 3429, 2850–2918, 1716, 1472, 1367, 1162, 1047, 956–963 and 718–730 cm^{-1} that ascribed to stretching vibration modes of OH groups, (CH_2) asymmetric stretching vibration, (C=O) stretching vibration of ester carbonyl group, (CH_2) bending vibration, (CH_2) symmetric vibration, C–O–C stretching vibration, –O–C–C stretching vibrations, –C–OH bending vibration of the carboxylic acid groups and (CH_2) rocking bending vibration, respectively [14, 33–35]. The existence of the IR peaks of the individual constituents (i.e., HDPE; PBS; HDPE-g-MA) in each curve in Fig. 1 proves the presence of each integrant separately, and hence, there is no chemical (i.e., only physical) interaction evolved between the components. The nonoccurrence of chemical interaction between such components was due to the high molecular weight of PBS (72,000) that makes it does not attack the ester groups of HDPE-g-MA due to its low chain mobility [36].

Table 2 IR peaks and their assignments for the as-synthesized blends

Peak wave number (cm^{-1})	Assignment	The peak is attributed to
3429–3430	Stretching vibration modes of OH groups	PBS
2328; 2850–2918	(CH_2) asymmetric stretching vibration	HDPE
1716	(C=O) stretching vibration of the ester carbonyl group	PBS and/or HDPE-g-MA
1472	(C–H) bending vibration	HDPE and/or HDPE-g-MA
1367	(CH_2) symmetric vibration	HDPE
1162	C–O–C stretching vibration	PBS
1047	–O–C–C stretching vibrations	PBS and/or HDPE-g-MA
956–963	–C–OH bending vibration of the carboxylic acid groups	PBS
718–730	(CH_2) rocking bending vibration	HDPE and/or PBS and/or HDPE-g-MA

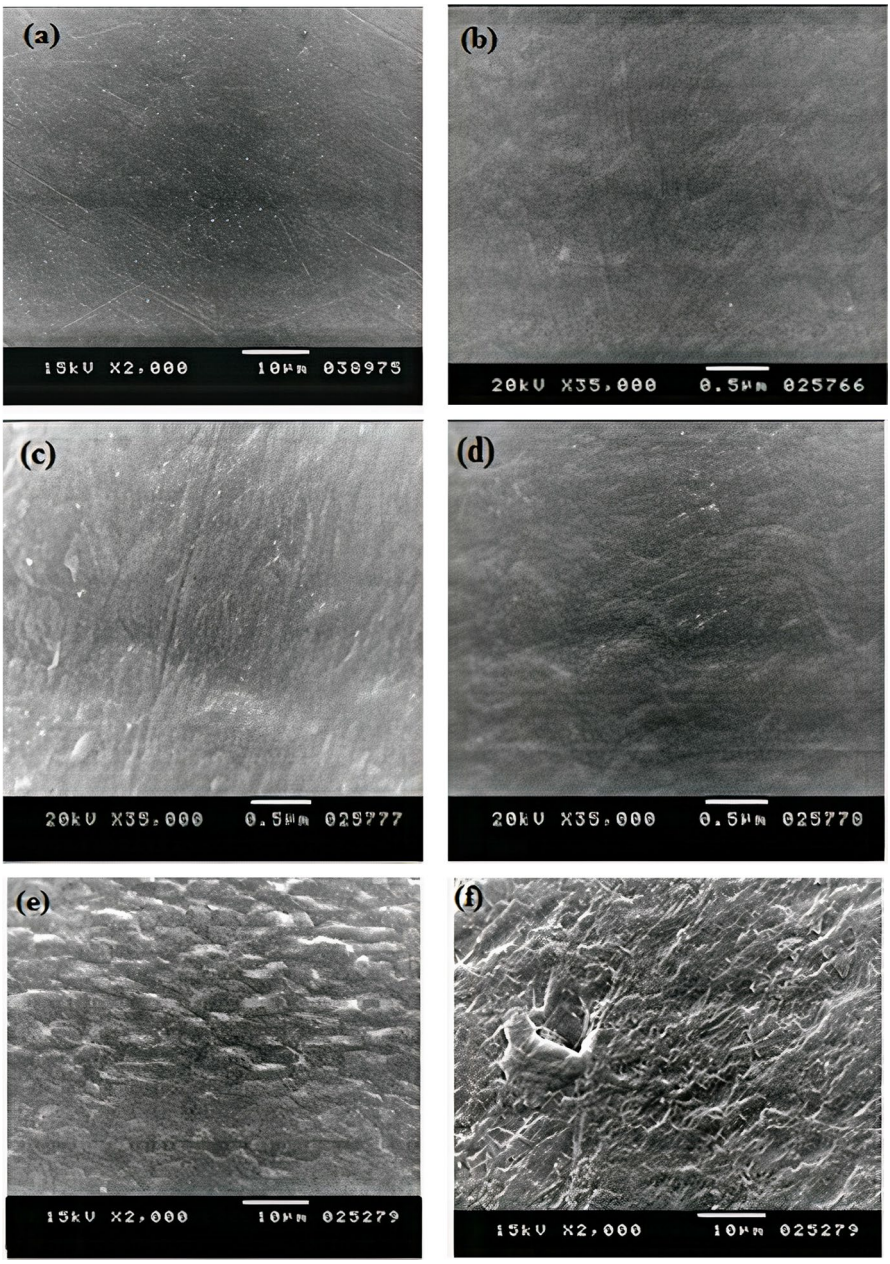

Fig. 2 SEM micrographs of **a** S0 **b** S11, **c** S12, **d** S14, **e** S21, **f** S22, **g** S24, **h** S41, **i** S42 and **j** S44 blends, respectively

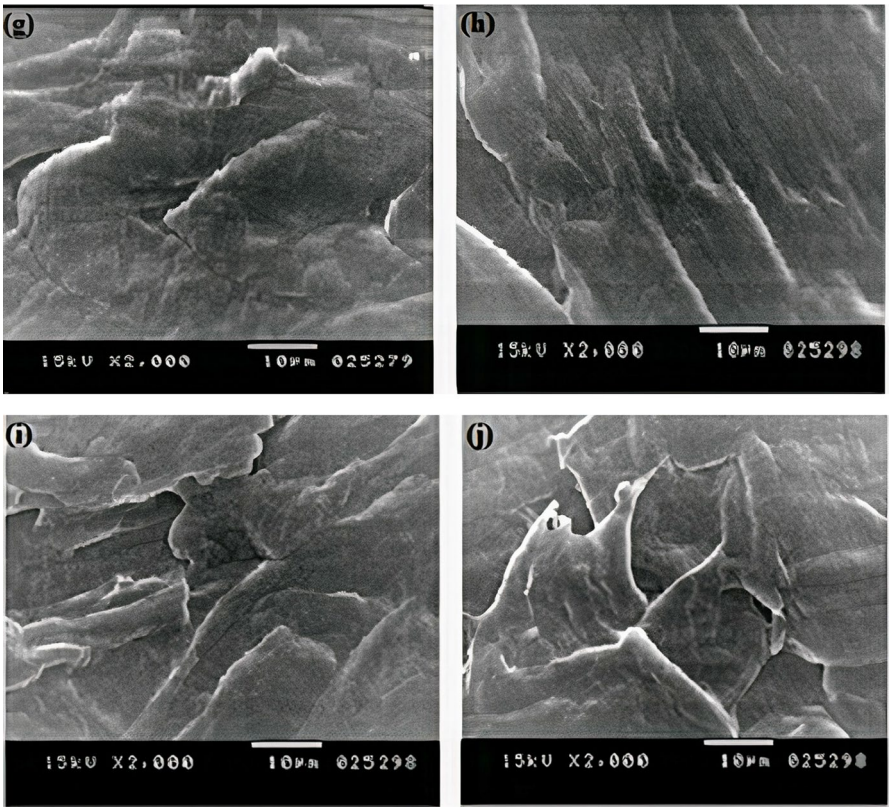

Fig. 2 (continued)

Phase morphology

SEM micrographs of HDPE (neat) and the as-prepared mixes are shown in Fig. 2a–j. Figure 2a indicates that HDPE has a homogenous, smooth and uniform surface. All composites that contain low weight percentages of HDPE-g-MA (i.e., (S11), (S21) and (S41)) show a good dispersion inside the HDPE matrix and give good smooth and homogeneous surface distribution. The possible linkage between the MA (of HDPE-g-MA) and ester group of PBS was responsible for this observation; but in the case of high HDPE-g-MA weight percentages, it is noted a bad dispersion inside the HDPE matrix which gives inhomogeneity to the surfaces of such composites. In the state of the high content of HDPE-g-MA, there was an inherent incompatibility between HDPE and PBS, so, the adhesion between the PBS and the HDPE is not good in the admixtures containing 4% HDPE-g-MA ((S14), (S24) and (S44)), which may be assigned to the high percentage of HDPE-g-MA that does not allow the dispersion of PBS inside the HDPE matrix. Conversely, there was a relatively positive dispersion of PBS through the HDPE matrix in the composites containing 1% HDPE-g-MA, which

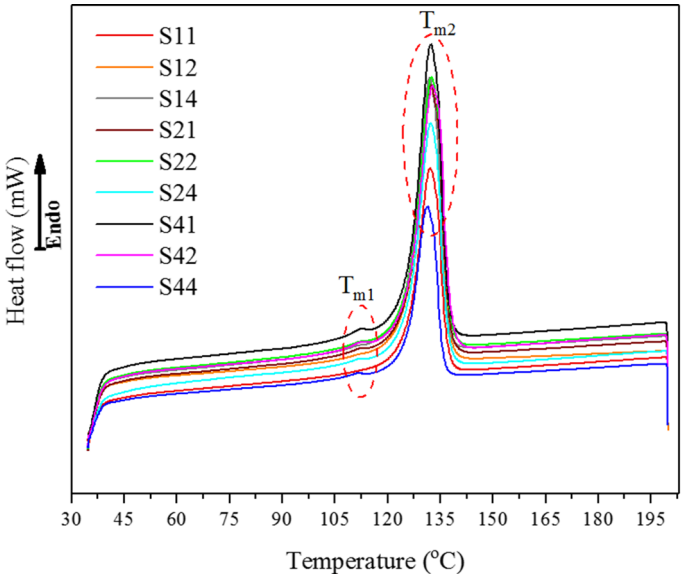

Fig. 3 DSC scans of the prepared composites

may be assigned to the improvement of the PBS dispersion in the HDPE matrix. As shown in Fig. 2, there is no interfacial adhesion between the components of the admixtures containing 4% HDPE-g-MA.

Thermal characteristics (crystallinity and melting behavior)

The DSC scans of the blends are exhibited in Fig. 3. The figure reveals two endothermic peaks in keeping with the melting process (T_m) as marked in

Table 3 Peak melting temperature (T_m), the heat of fusion (ΔH) and the crystallinity percentage (χ_c %) of both the pure polymers used in the study and of the prepared blends

Sample	T_{m1} (°C) ± 0.522	T_{m2} (°C) ± 1.88	ΔH (J/g)	χ_c %
HDPE (S0)	–	136.20	184.60	63.60
PBS	113.37	–	91.93	57.40
HDPE-g-MA	–	137.60	139.52	48.11
S11	111.70	132.10	181.28	62.52
S12	111.82	132.00	173.00	59.65
S14	111.81	132.00	149.20	51.44
S21	112.74	132.50	180.61	62.28
S22	112.52	132.50	172.95	59.63
S24	112.29	132.10	164.68	50.58
S41	112.67	132.78	174.40	60.13
S42	112.80	132.27	172.26	59.44
S44	111.90	131.30	107.10	36.93

Fig. 4 Stress–strain curves of **a** S0, **b** S11, **c** S22, **d** S44 blends, respectively (for each figure, the test was performed more than one time for each specimen, respectively, and the average was taken) ▶

the figure. The first melting peak temperature (T_{m1}) was in the domain of 111.70–112.80 ± 0.522 °C that is in agreement with the melting of PBS. The second distinct melting peak (T_{m2}) was in the limits 131.30–132.78 ± 1.88 °C. This peak is ascribed to the melting of HDPE and/or HDPE-g-MA (which overlapped because of the convergence between them). Similarly, the ΔH decreased from 181.28 for S11 to 107.10 J/g for S44 and the crystallinity percentage (χ_c %) decreased from 62.52 for S11 to 36.93% for S44 as tabulated in Table 3. The results are in good harmony with the ones found by Roumeli et al. [34]. The existence of two melting peaks for each of the DSC scans of the prepared blends and the difference in the melting temperatures between the polymers before and after the blending proves that there is no chemical interaction evolved between the components as confirmed from IR results. The crystallinity reduction may be because of two reasons: firstly, adding a semicrystalline component (like PBS) with similar or smaller crystallinity degrees to the matrix (as in the ongoing case) which tends to decrease the mobility and flexibility and hence the crystallinity of the composites and disrupts the long-chain order in various zones of HDPE matrix. This justification was consistent with the explication reported in other literature [37]. Secondly, adding a high M_{Wt} component just like the PBS (72,000) has a great impact on the crystallinity in keeping with the repetition-nucleation theory (that states the relevance between M_{Wt} and the crystallinity) [38]. In the ongoing case, longer chains may form a loop to interfere with chain folding and subsequently decrease the final degree of crystallinity. This complies with the same reported by various authors [23, 35, 39].

Table 4 Tensile strengths at yield and at the break, elongation (%), the Young's modulus (*E*) and impact strength of the synthesized blends

Sample	Tensile strength at yield ± 0.3 (MPa)	Tensile strength at break ± 0.58 (MPa)	Elongation ± 76.09 (%)	*E* (MPa)	Impact strength ± 11.23 (KJ/m^2)
S0	26	6.53	1035	700	117.80
S11	27	8.68	1317	500	147.70
S12	26	7.89	1232	480	127.00
S14	26	7.37	1208	450	123.50
S21	26	7.27	1272	410	148.10
S22	26	7.20	1223	390	124.50
S24	26	7.10	1164	370	111.80
S41	26	7.22	1183	350	130.10
S42	26	6.89	1135	330	130.00
S44	26	6.75	1126	290	137.70

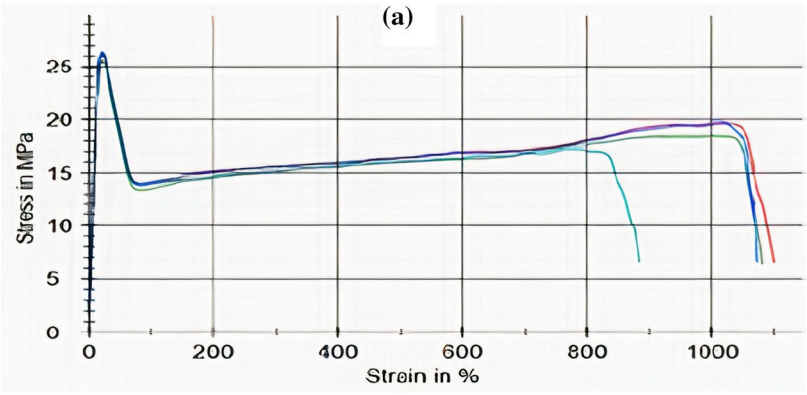
(a)
Stress in MPa
0
5
10
15
20
25
0
200
400
600
800
1000
Strain in %

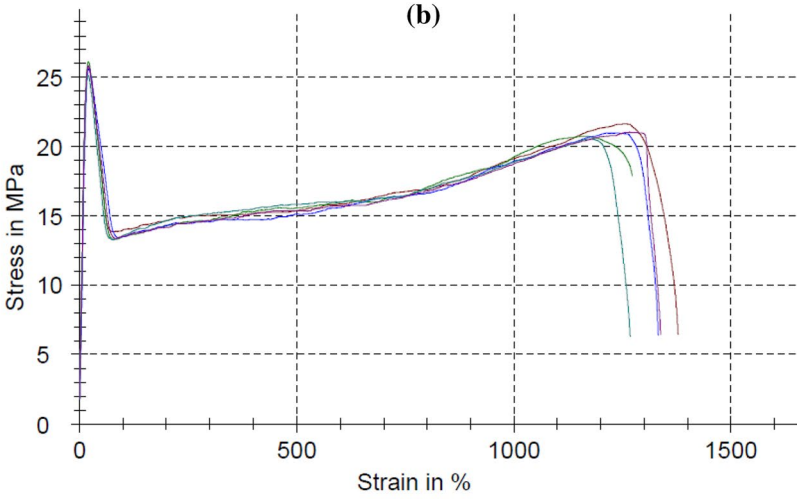
(b)
Stress in MPa
0
5
10
15
20
25
0
500
1000
1500
Strain in %

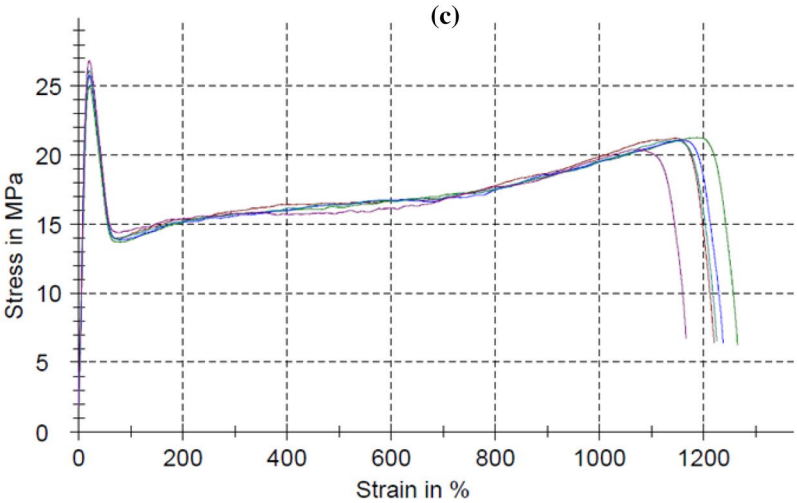
(c)
Stress in MPa
0
5
10
15
20
25
0
200
400
600
800
1000
1200
Strain in %

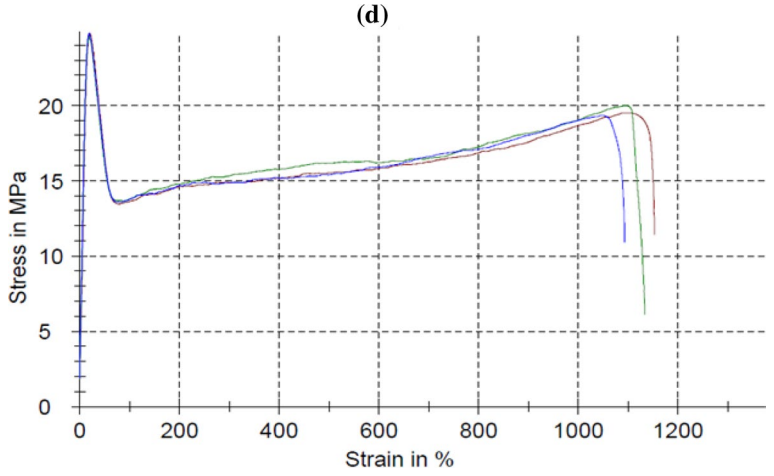

Fig. 4 (continued)

Mechanical properties

Tensile strength and elongation

The tensile strength at yield, the tensile strength at break, elongation at break and yield stress of the specimens were determined to examine the blends' stiffness and they are recorded in Table 4. The tensile strength at yield of HDPE (as in sample S0) and all the other samples (S11–S44) was approximately constant. Figure 4a–d shows different stress–strain curves of the synthesized composites. For each specimen, the test was performed at least three times and the average was taken.

Figure 4a illustrates the stress–strain curve of the neat HDPE. The curve shows a severe increment in the elastic region when the tensile strength was 26 ± 0.3 MPa. After the yield point, the curves start to behave plastically and show elongation percentages with an average of $1035\% \pm 76.09$ until they hit the breaking point with an average strength of 6.53 ± 0.58 MPa.

As tabulated in Table 4, the elongation and tensile strengths increase from 1035 for the S0 sample to $1317\% \pm 76.09$ for the S11 sample and from 6.53 for the S0 sample to 8.68 ± 0.58 MPa for the S11 sample, respectively. This might be an effect of the well interfacial adhesion between the PBS domain and HDPE matrix which is promoted by physical interaction between the HDPE-g-MA and PBS, and also by the physical entanglement of molecular chains between HDPE matrix and HDPE backbones of HDPE-g-MAH. After that, the elongation and tensile strengths lowered with growing HDPE-g-MA contents through the composites. The curve (b as a representative of this group) presents a little increment in the elastic region and the tensile strength point which was at 27 ± 0.3 MPa. After the yield point, the curve starts to behave plastically and shows an elongation percentage with an average of $1317\% \pm 76.09$ till it hits the breaking point with an average strength of 8.68 ± 0.58 MPa.

The tensile strength point was also at 26 ± 0.3 MPa. After the yield point, the curve (*d* as a representative of this group) starts to behave plastically and shows an elongation percentage with an average of 1126% ± 76.09 till it hits the breaking point with an average strength of 6.75 ± 0.58 MPa. The great improvement of the elongation of HDPE might be assigned to the attendance of the plasticizer PBS which is acting on HDPE as a spacer and increases the free volumes. This leads to HDPE becoming softer and weaker and permits higher elongation. The plasticizing effect is accompanied by the incursion of PBS to the polymer matrix is in an agreement with DSC measurements (Table 3) of the as-prepared system and in agreement with that has been stated previously in [40, 41]. Decreasing the tensile strength and elongation values through the system may be as a result of increasing HDPE-g-MA that decreased the plasticizing effect of the plasticizer PBS.

Young's modulus (*E*)

(*E*) of the HDPE/PBS/HDPE-g-MA composites decreases by increasing PBS and PE-g-MA contents in the admixtures as given in Table 4. (*E*) decreases from 700 Mpa for neat HDPE to 290 Mpa for S44 blend. Regarding each group of the series, (*E*) decreases from 700 Mpa for the neat PE to 500 Mpa for S11, 480 Mpa for S12 and 450 Mpa for S14, respectively. Also, for the second group of concentrations, (*E*) decreases from 700 Mpa for S0 to 410 Mpa for S21, 390 MPa for S22 and 370 MPa for S24, respectively. Regarding the final group of the concentrations, (*E*) decreases from 700 Mpa for S0 to 350 Mpa for S41, 330 Mpa for S42 and 290 Mpa for S44, respectively.

This general decrease in (*E*) by increasing PBS and HDPE-g-MA contents in HDPE/PBS/ HDPE-g-MA composites might be assigned to adding of lower Young's modulus polymers (501 MPa for PBS and 340 MPa for HDPE-g-MA) to higher HDPE (700 MPa) Young's modulus.

Impact strength

The impact strength of the prepared composites increased by increasing PBS and HDPE-g-MA contents as recorded in Table 4. The results offer a general upgrade in the toughness from 117.80 for S0 to 147.70 kJ/m^2 in S11, 124.50 kJ/m^2 in S22 and 137.70 (± 11.23) kJ/m^2 in S44. All the impact strengths of the HDPE/PBS/ HDPE-g-MA composites were higher than that of the neat HDPE. This increase might be owing to the insertion of PBS and HDPE-g-MA to the HDPE matrix which enhances the toughness of HDPE by the inherent flexibility of PBS [42]. Also, this increase in impact strength with the merger of HDPE-g-MA may be ascribed to two reasons; firstly, the capability of HDPE-g-MA to introduce a degree of cross-linking into the matrix. Secondly, the increase in the interfacial adhesion in the zones of stress concentration (i.e., in the position where the pendulum impacts the specimen) enabled the distortion to happen simply and eased shear yielding [43].

Hardness test

The hardness of the existing system increased from 57.3 (for neat HDPE) to 57.4 (for S11), 60.2 (for S22) and 61.1 (for S44). This may be relevant to the increment in stiffness that happened by the existence of rigid filler (i.e., HDPE-g-MA) in the matrix [44]; so, the insertion of HDPE-g-MA led to greater compatibility and stronger interfacial interaction between PBS and HDPE, leading to this rising in the hardness.

Physical property analysis

Melt Flow Index (MFI)

MFI is a measure of the easiness of flowing the melt of thermoplastic polymer. It is the quantity of polymer, in grams, flowing in ten minutes across a capillary of a certain diameter and length by a pressure employed through fixed alternative gravimetric weights for predetermined temperatures. MFI helps in determining the force and temperature needed during the processing to maintain consistent product quality without creating waste material. MFI at 190 °C for HDPE and all the synthesized blends are revealed by Table 5. From the table, it is obvious that adding 1% of PBS in S11, S12 and S14 composites caused increasing the mixture's viscosity and consequently a reduction of MFI to 6.99, 7.49 and 7.50 g/10 min, respectively, relative to the pure HDPE (8.49 g/10 min). Doubling the PBS percentage to 2% in samples S21, S22 and S24 increased MFI to 7.70, 7.89 and 7.90 g/10 min, while increasing the PBS percentage to 4% raised MFI to 8.00 and 8.10 in samples S41 and S42 and to 8.10 g/10 min for S44, respectively. The insertion of a biodegradable polymer such as PBS to HDPE increases the viscosity which is also in accordance with decreasing MFI results for the different composites. For processing purposes, the above-mentioned results affirmed that blending HDPE with biopolymers leads

Table 5 Melt Flow index (MFI) and water absorption data of the prepared blends

Sample	MFI (g/10 min)	Water absorption (%)/duration ± 0.0001					
		(1 day)	(1 week)	(3 weeks)	(5 weeks)	(7 weeks)	(9 weeks)
S0	8.49	0.002	0.002	0.002	0.002	0.002	0.002
S11	6.99	0.002	0.003	0.003	0.003	0.003	0.003
S12	7.49	0.003	0.004	0.005	0.005	0.005	0.005
S14	7.50	0.005	0.006	0.007	0.007	0.007	0.007
S21	7.70	0.004	0.005	0.006	0.006	0.006	0.006
S22	7.89	0.006	0.007	0.007	0.007	0.007	0.007
S24	7.90	0.007	0.008	0.008	0.008	0.008	0.008
S41	8.00	0.008	0.009	0.010	0.010	0.010	0.010
S42	8.10	0.010	0.011	0.012	0.012	0.012	0.012
S44	8.10	0.014	0.017	0.018	0.018	0.018	0.018

to extruding the materials more easily. The reduction was related to the decrement in the mobility of the chains around the PBS which decreased the polymer flow into the mold that then affects the polymer processing [45].

Water absorption test

The water absorption data of the HDPE/PBS/HDPE-g-MA composites at the soaking time of 9 weeks are demonstrated in Table 5. The hydrophobic neat HDPE sample absorbed only 0.002% during the 9 weeks of water soaking, while the water uptake of all the blends increased slightly up to 0.018% for the S44 blend. This slight increase is basically due to the addition of PBS that has a hydrophilic nature and low crystalline nature which consequently increased the water absorption [42].

Oxidative induction time (OIT)

OIT is a proportional scale of a material's resistance to oxidative decomposition; it is stated by the thermoanalytical computation of the time interlude to the beginning of exothermic oxidation of a matter at a set temperature in an oxygen atmosphere. Exposure of HDPE to the heat, oxygen and shear of processing without antioxidants additives can cause chain scission and shortening of molecular chains. Upon subjection to oxygen, auto-oxidation is initiated by the generation of free radicals (reactive molecular species with unpaired electrons). Autoxidation is a circular process except when it interferes with an antioxidant that gradually leads to a rise in the deterioration of the polymer because of the resultant fragments [46, 47]. These radicals can degrade HDPE by free propagation mechanism via breaking of its polymeric chains or cross-linking between chains. Exposure to oxygen is becoming the greatest at the surfaces of the HDPE products which are the most visibly affected due to the creation of cracked, powdery and/or chalked surfaces [48].

In the existence of oxygen, autoxidation develops over a succession of initiation, propagation and branching chain reactions:

1. Heat, shear and catalyst residues tend to strip hydrogen from the polymer chain (RH) and form alkyl free radicals (R●).
2. Oxygen joins with the free radicals to install novel reactive species made up of peroxy radicals and hydroperoxides and other species (H_2O, H_2, H_2O_2).
3. $\left(O_2 + R\bullet \rightarrow ROO\bullet\right)$
4. The hydroperoxides (ROOH) are themselves reactive and form new free radical species, such as hydroxy and alkoxy radicals
5. $(ROOH \longrightarrow \bullet OH + RO\bullet)$ [49].

Antioxidants interfere with the HDPE matrix and slow down (or nearly stop) the propagation of free radical reactions that break the HDPE chains. Primary antioxidants do this by "scavenging" or consuming the free radicals, while secondary antioxidants react with secondary hydroperoxide species that are formed during

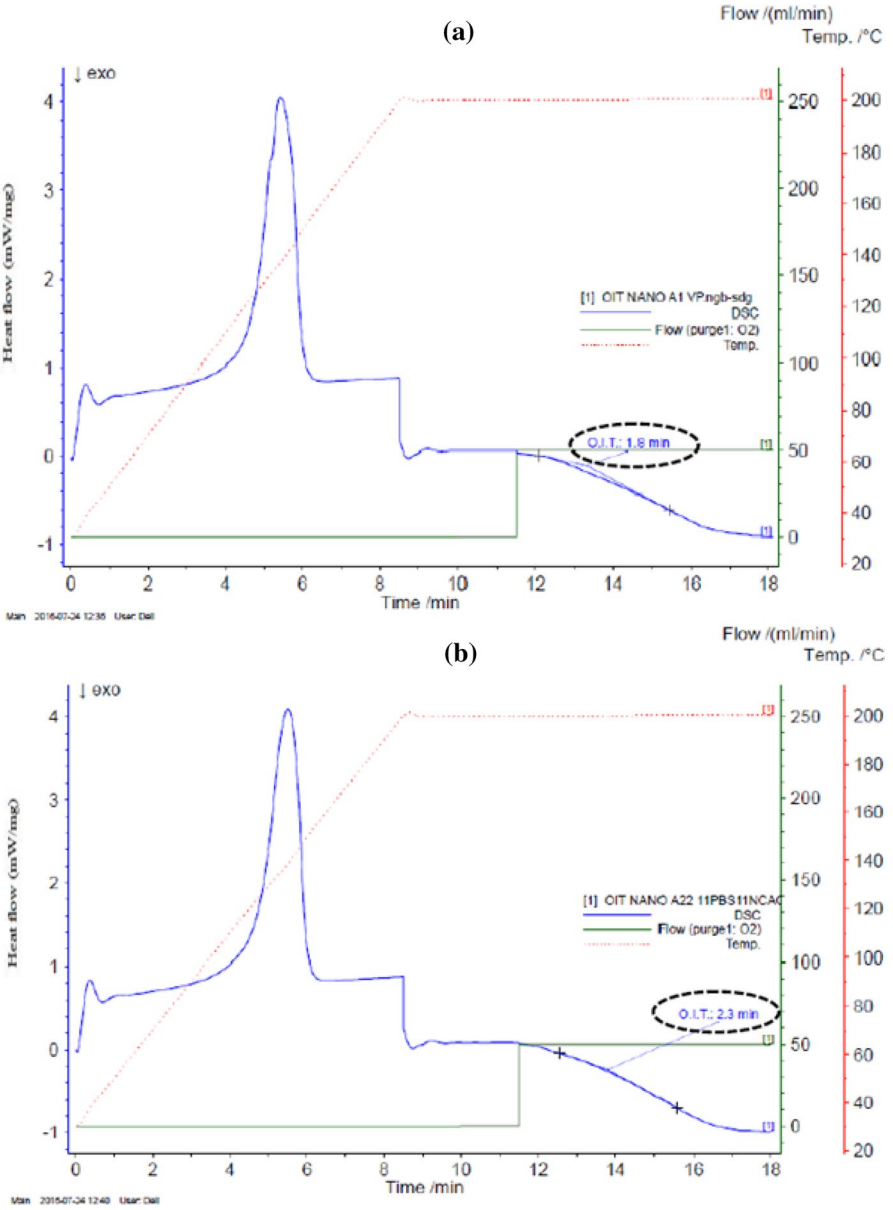

Fig. 5 Oxidation induction time of **a** S0, **b** S11, **c** S44 and **d** S 6070UA blends

autoxidation and prevent them from further degrading the polymer and increase the heat stability [50].

Oxidative stability of neat HDPE (S0), its composites (S11, S44) and the commercial HDPE 6070 were investigated by the OIT experiment as revealed by Fig. 5a–d.

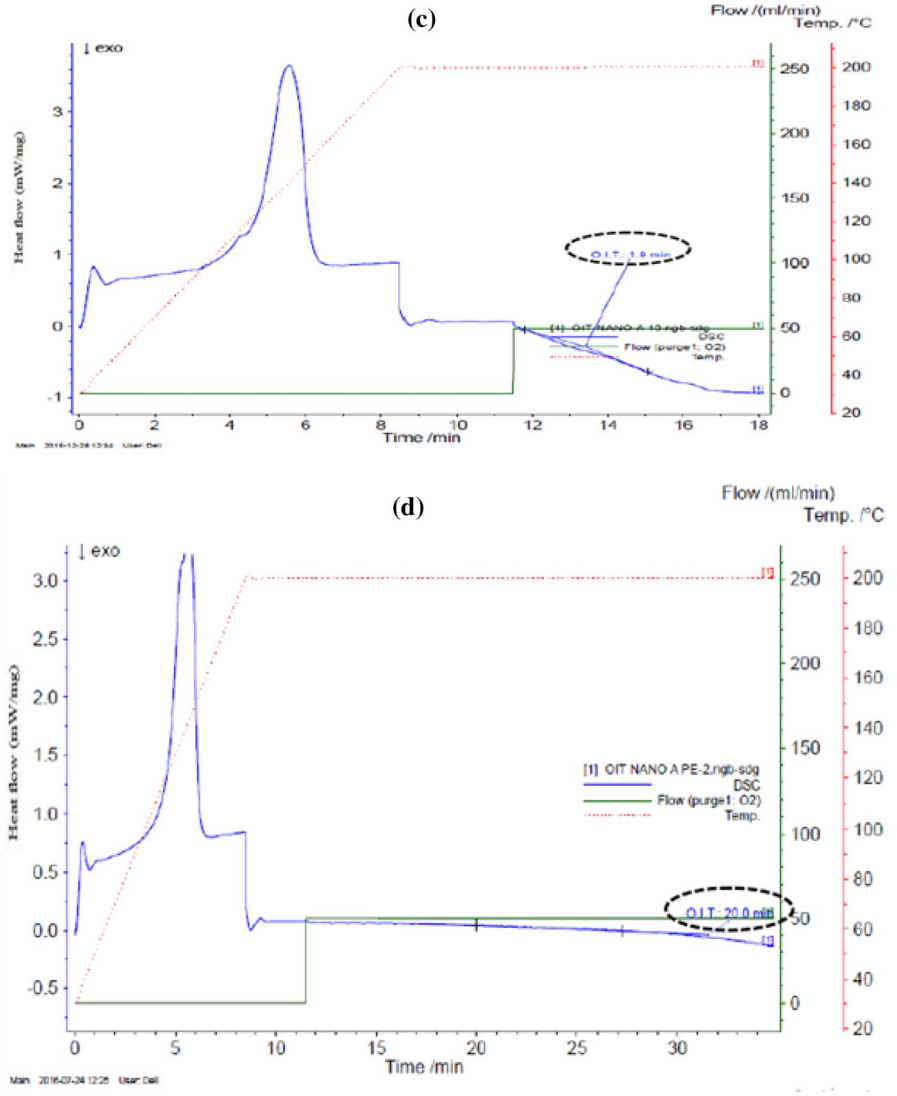

Fig. 5 (continued)

The results present that the time of oxidation induction changed from 1.8 min (for S0) to 2.3 min (for S11); in the S44 blend, the thermal oxidation stability decreased and the OIT decreased to 1.9 min.

In the case of the commercial HDPE with antioxidant additives (Irganox 1010, Irganox 1076) in the sample S 6070UA, OIT reached 20 min. So, it can be inferred that the introducing of HDPE-g-MA with PBS cannot prevent HDPE oxidation and it is a need to add primary and secondary antioxidants to protect the composite from oxidative degradation.

Table 6 Biodegradation data of the prepared composites

Sample	Weight loss %/duration ± 0.0001		
	1 Month	2 Months	4 Months
S0	0	0	0
S11	0	0.02	0.04
S12	0	0.02	0.05
S14	0	0.03	0.05
S21	0	0.03	0.06
S22	0	0.04	0.06
S24	0	0.05	0.08
S41	0	0.07	0.09
S42	0	0.07	0.10
S44	0	0.09	0.12

Biodegradation properties

The biodegradability of the different composites can be checked using the soil interment method by determining the weight drop percentage in a specific duration and SEM micrographs. Table 6 shows the weight loss percentages of HDPE/PBS/HDPE-g-MA composites for 4 months.

It is essential to remind that only biodegradation is measured without any consideration of the UV degradation which is also of major importance in the state of HDPE. The weight drop of the synthesized samples after burial in the soil for 4 months was determined by the biogeophysical test that can present a realistic because of the soil humidity, temperature and microorganisms [51]. The samples continuously degrade with rising number of months which suggests that microorganisms consume PBS and create pores in the PE matrix [52]. All composites exhibit greater weight losses in contradiction of pure HDPE that showed there is no effect in weight loss even after 4 months as presented in Table 6 and confirmed previously by Abdel-Hakim and Mourad [53]. In sample S11, the weight drop % reached 0.04% and 0.05% for S12 and S14 samples, respectively, after 4 months. By doubling the percentage of PBS for the blends S21 and S22, the weight loss % increased to 0.06% and increased again to 0.08% for S24 after 4 months. In the case of S41, S42 and S44, the weight drop % increased to 0.09, 0.10 and 0.12% (± 0.0001) after 4 months.

The presence of PBS and HDPE-g-MA increases the susceptibility of the blends to biodegradability where PBS is biodegradable polyester that can be influenced by the act of microorganisms in the soil [42]. The enhanced degradation of the blends compared to HDPE can be demonstrated by the initiation of microbial deterioration of PBS chains. Therefore, as the PBS quantity increases, the biodegradation increases. Also, as the HDPE-g-MA concentration increases the moisture absorption and the swelling increase too leading to faster biodegradation [54, 55].

HDPE is deteriorated by fungal adhesion; on the other side, PBS is protected by HDPE (HDPE delays the degradation speed of the PBS or any matrix in which the PBS exists), which controls the biodegradation process and makes the PBS fewer

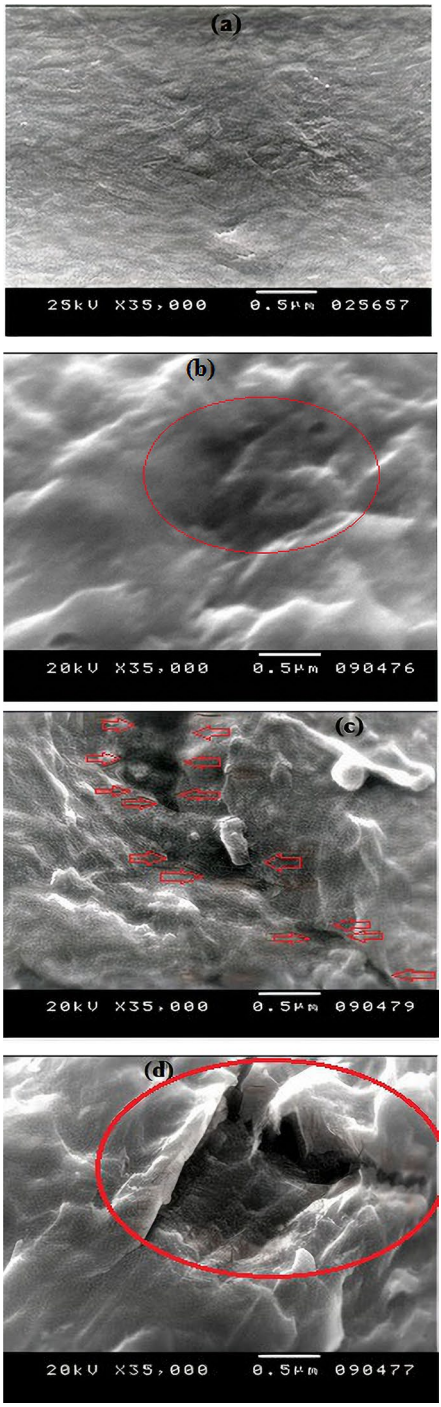

Fig. 6 SEM micrographs after degradation of **a** S0, **b** S11, **c** S22, **d** S44 blends (the pores resulted from degradation are marked in each picture)

susceptible to microbial attack. Despite that and the little quantity of PBS inside the HDPE matrix, it gives considerable degradation results after 4 months. The examination of SEM's for the S0 and the degraded S11, S22 and S44 mixes is pictured in Fig. 6. Figure 6a shows that there is no appearance of holes or fungal growth in sample S0 and this may be a result of the HDPE resistance for the microbial growth on its surface. Figure 6b–d shows that the surfaces of S11, S22 and S44 mixes have holes, cracks and rough structures. These morphological variances indicate the microbial action on the matrix surface. Morphological changes by the act of degradation may occur at locations of instability just like chain ends, chain folds and the edge of the crystals where the chain mobility looks to be higher. The degradation of lamellar edges may result in lamellar thinning and allow the melting to occur at slightly lower temperatures than the original crystals [56] which achieved in the present system as revealed by T_m values in Table 3.

Conclusion

Blends of HDPE, PBS and HDPE-g-MA were prepared by adding 1, 2 and 4 wt% of PBS to the HDPE with the participation of similar percentages of HDPE-g-MA.

The FTIR spectra proved that the HDPE, PBS and HDPE-g-MA (the three ingredients of the composite) were present individually in all the prepared mixtures. The SEM micrographs proved that the composites containing low percentages of HDPE-g-MA had good diffusion throughout the HDPE matrix and provided a smooth feel to the surface along with a homogenous surface distribution. DSC results showed a little impact on the melting temperatures and the merger of 1%, 2% and 4% PBS led to a decrease in the crystallinity percentage. When the percent of the HDPE-g-MA increased, the interfacial adhesion between PBS and HDPE decreased. It should also be noted that increasing the PBS content improved the mechanical properties of the neat HDPE. The elongation percentage at break (at the lowest HDPE-g-MA content) increased by virtue of the high flexibility of PBS and decreasing the interfacial adhesion between composites components, while the yield tensile strength of all blends was nearly the same in resembling that of neat HDPE. The toughness of the mixtures was increased by the behavior of the elongation for the same yield stresses by increasing PBS and HDPE-g-MA percentages. The impact strength of HDPE was increased by 25.6% for the S11 and then decreased with the increase in both PBS and HDPE-g-MA. The hardness of HDPE was also increased by rising the contents of both PBS and HDPE-g-MA.

The MFI of the mixes was increased with the rising of the PBS wt.%. The water absorption of the prepared blends insignificantly increased as a result of the hydrophilic nature of PBS and the decrease in the crystallinity percentage of the mixtures which gave a chance for water to penetrate at a larger rate. The OIT of the neat HDPE was not affected by adding PBS or HDPE-g-MA. All composites could not resist oxidative degradation. Therefore, as the PBS bulk increases, the biodegradation increases. Also, as the HDPE-g-MA bulk increases, the moisture absorption and the swelling increase too that result in faster biodegradation. For future works, the addition of HDPE-g-MA generally deteriorates the properties of the blend when

added in large quantities as indicated in the present system or as in the previous works [57, 58]. For that reason, it is recommended that HDPE-g-MA percent should not exceed 1 wt.% for obtaining better properties.

References

1. Borrowman CK, Johnston P, Adhikari R, Saito K, Patti AF (2020) Environmental degradation and efficacy of a sprayable, biodegradable polymeric mulch. Polym Degrad Stab 175:109126. https://doi.org/10.1016/j.polymdegradstab.2020.109126
2. Prabhu R, Devaraju A (2020) Recent review of tribology, rheology of biodegradable and FDM compatible polymers. Mater Today. https://doi.org/10.1016/j.matpr.2020.09.509
3. Anjana K, Hinduja M, Sujitha K, Dharani G (2020) Review on plastic wastes in marine environment–biodegradation and biotechnological solutions. Mar Pollut Bull 150:110733. https://doi.org/10.1016/j.marpolbul.2019.110733
4. Chaudhary AK, Vijayakumar RP (2020) Effect of chemical treatment on biological degradation of high-density polyethylene (HDPE). Environ Dev Sustain 22:1093–1104. https://doi.org/10.1007/s10668-018-0236-6
5. Abd El-Rahman KM, Ali SF, Khalil AI, Kandil S (2020) Influence of poly (butylene succinate) and calcium carbonate nanoparticles on the biodegradability of high density-polyethylene nanocomposites. J Polym Res 27:1–21. https://doi.org/10.1007/s10965-020-02217-y
6. Gautam R, Bassi AS, Yanful EKA (2007) A review of biodegradation of synthetic plastic and foams. Appl Biochem Biotechnol 141:85–108. https://doi.org/10.1007/s12010-007-9212-6
7. Tokiwa Y, Calabia BP (2007) Biodegradability and biodegradation of polyesters. J Polym Environ 15:259–267. https://doi.org/10.1007/s10924-007-0066-3
8. Miller E (1996) Introduction to plastics and composites: mechanical properties and engineering applications. M. Dekker, New York
9. Nowak B, Paja k, J., Drozd-Bratkowicz, M. and Rymarz, G. (2011) Microorganisms participating in the biodegradation of modified polyethylene films in different soils under laboratory conditions. Int Biodeterior Biodegradation 65:757–767. https://doi.org/10.1016/j.ibiod.2011.04.007
10. Maul J, Frushour BG, Kontoff JR, Eichenauer H, Ott KH, Schade C (2007) Ullmann's encyclopedia of industrial chemistry. Wiley, New Jersey. https://doi.org/10.1002/14356007.a21_615.pub
11. Darshan TG, Veluri S, Kartik B, Yen-Hsiang C, Fang-Chyou C (2019) Poly (butylene succinate)/high density polyethylene blend-based nanocomposites with enhanced physical properties–Selectively localized carbon nanotube in pseudo-double percolated structure. Polym Degrad Stab 163:185–194. https://doi.org/10.1016/j.polymdegradstab.2019.03.009
12. Charles EC (2012) Introduction to polymer chemistry. CRC Press, Florida
13. EC. Charles (2010) Carraher's polymer chemistry: CRC Press; Florida.
14. Viljoen WD, Labuschagne FJ (2020) The thermal stability of highly filled high-density polyethylene quaternary composites: Interactive effects and improved measures. Polym Test 85:106424. https://doi.org/10.1016/j.polymertesting.2020.106424
15. Behera K, Sivanjineyulu V, Chang YH, Chiu FC (2018) Thermal properties, phase morphology and stability of biodegradable PLA/PBSL/HAp composites. Polym Degrad Stab 154:248–260. https://doi.org/10.1016/j.polymdegradstab.2018.06.010
16. Sivanjineyulu V, Chang YH, Chiu FC (2017) Characterization of carbon nanotube-and organoclay-filled polypropylene/poly (butylene succinate) blend-based nanocomposites with enhanced rigidity and electrical conductivity. J Polym Res 24:130. https://doi.org/10.1007/s10965-017-1289-1
17. Xu J, Guo BH (2010) Microbial succinic acid, its polymer poly(butylene succinate) and applications. Berlin 14:347–388. https://doi.org/10.1007/978-3-642-03287_5_14
18. Babu RO, Connor K, Seeram R (2013) Current progress on bio-based polymers and their future trends. Prog Biomater 2:8. https://doi.org/10.1186/2194-0517-2-8
19. Shokri E, Yegani R, Heidari S, Shoeyb Z (2015) Effect of PE-g-MA compatibilizer on the structure and performance of HDPE/EVA blend membranes fabricated via TIPS method. Chem Eng Res Des 100:237–247. https://doi.org/10.1016/j.cherd.2015.05.025
20. Cano S, Gooneie A, Kukla C, Rieß G, Holzer C, Gonzalez-Gutierrez J (2020) Modification of interfacial interactions in ceramic-polymer nanocomposites by grafting: morphology and properties for

powder injection molding and additive manufacturing. Appl Sci 10:1471. https://doi.org/10.3390/app10041471
21. Huang J, Cui C, Yan G, Huang J, Zhang MA (2016) Study on degradation of composite material PBS/PCL. Polym Polym Compos 24:143–148. https://doi.org/10.1177/096739111602400209
22. Yang J, Qin G, Liang J (2014) Flow properties and extensional viscosity prediction of high-density polyethylene and poly (butylene succinate) blends. J Thermoplast Compos 29:479–493
23. Aontee A, Sutapun WA (2013) A study of compatibilization effect on physical properties of poly(butylene succinate) and high density polyethylene blend. Adv Mat Res 699:51–56
24. ASTM Standard D3418, 2015, "Standard Test Method for Transition Temperatures and Enthalpies of Fusion and Crystallization of Polymers by Differential Scanning Calorimetry", ASTM International, West Conshohocken, PA, 2015, DOI: https://doi.org/10.1520/D3418-15, www.astm.org
25. ASTM Standard D638 (2014) Standard test method for tensile properties of plastics", ASTM International, West Conshohocken, PA, 2014, DOI: https://doi.org/10.1520/D0638-14, www.astm.org
26. ASTM Standard D4812 (2019,) Standard test method for unnotched cantilever beam impact resistance of plastics, ASTM International, West Conshohocken, PA, 2019, DOI: https://doi.org/10.1520/D4812-19, www.astm.org
27. ASTM Standard D2240 (2015) Standard test method for rubber property—durometer hardness, ASTM International, West Conshohocken, PA, 2015, DOI: https://doi.org/10.1520/D2240-15, www.astm.org
28. Chanda M (2017) Plastics technology handbook. CRC Press
29. ASTM Standard D1238 (2013) Standard Test Method for Melt Flow Rates of Thermoplastics by Extrusion Plastometer, ASTM International, West Conshohocken, PA, 2013, DOI: https://doi.org/10.1520/D1238-13, www.astm.org
30. ASTM Standard D570–98 (2018) Standard Test Method for Water Absorption of Plastics, ASTM International, West Conshohocken, PA, 2018, https://doi.org/10.1520/D0570-98R18, www.astm.org
31. ASTM Standard D3895–07 (2007) Standard test method for oxidative-induction time of polyolefins by differential scanning calorimetry, ASTM International, West Conshohocken, PA, 2007, https://doi.org/10.1520/D3895-07, www.astm.org
32. ASTM Standard D5988–18 (2018) Standard test method for determining aerobic biodegradation of plastic materials in soil, ASTM International, West Conshohocken, PA, 2018, https://doi.org/10.1520/D5988-18, www.astm.org
33. Mehrabzadeh M, Kamal MR, Quintanar G (2009) Maleic anhydride grafting onto HDPE by in situ reactive extrusion and its effect on intercalation and mechanical properties of HDPE/Clay nanocomposites. Iran Polym J 18:833–842
34. Roumeli E, Terzopoulou Z, Pavlidou E, Chrissafis K, Papadopoulou E, Athanasiadou E, Triantafyllidis K, Bikiaris DN (2015) Effect of maleic anhydride on the mechanical and thermal properties of hemp/high-density polyethylene green composites. J Therm Anal Calorim 121:93–105. https://doi.org/10.1007/s10973-015-4596-y
35. Kim HS, Lee BH, Choi SW, Kim S, Kim HJ (2007) The effect of types of maleic anhydride-grafted polypropylene (MAPP) on the interfacial adhesion properties of bio-flour-filled polypropylene composites. Compos Part A Appl Sci Manuf 38:1473–1482
36. Lim KY, Kim BC, Yoon KJ (2002) The effect of molecular weight of polycaprolactone on the ester interchange reactions during melt blending with poly(ethylene terephthalate). Polym J 34:313–319. https://doi.org/10.1295/polymj.34.313
37. Monteiro MS, Cucinelli Neto RP, Santos IC, Silva EO, Tavares MI (2012) Inorganic-organic hybrids based on poly (ε-Caprolactone) and silica oxide and characterization by relaxometry applying low-field NMR. Mater Res 15:825–832. https://doi.org/10.1590/S1516-14392012005000121
38. Yeh CC, Chen CN, Li YT, Chang CW, Cheng MY, Chang HI (2011) The effect of polymer molecular weight and UV radiation on physical properties and bioactivities of PCL films. Cell Polym 30:261–276. https://doi.org/10.1177/026248931103000503
39. Jenkins MJ, Harrison KL (2006) The effect of molecular weight on the crystallization kinetics of polycaprolactone. Polym Adv Technol 17:474–478. https://doi.org/10.1002/pat.733
40. Rahmah M, Nurazzi NM, Nordyana AF, Anas SS (2017) Effect of epoxidised soybean oil loading as plasticiser on physical, mechanical and thermal properties of polyvinylchloride. IOP Conf Ser Mater Sci Eng 223:012048. https://doi.org/10.1088/1757-899X/223/1/012048
41. Bhatia A, Gupta RK, Bhattacharya SN, Choi HJ (2007) Compatibility of biodegradable poly (lactic acid) (PLA) and poly (butylene succinate) (PBS) blends for packaging application. Korea-Aust Rheol J 19:125–131

42. Chuayjuljit S, Kongthan J, Chaiwutthinan P, Boonmahitthisud A (2018) Poly (vinyl chloride)/Poly (butylene succinate)/wood flour composites: physical properties and biodegradability. Polym Compos 39:1543–1552. https://doi.org/10.1002/pc.24098
43. Ahmad I, Fern LP (2006) Effect of PE-g-MA-compatibilizer on the morphology and mechanical properties of 70/30 HDPE/ENR blends. Polym Plast Technol Eng 45:735–739. https://doi.org/10.1080/03602550600611271
44. Obasi HC (2015) Peanut husk filled polyethylene composites: effects of filler content and compatibilizer on properties. J Polym. https://doi.org/10.1155/2015/189289
45. Sepet H, Tarakcioglu N, Misra RD (2016) Determination of the mechanical, thermal and physical properties of nano-$CaCO_3$ filled high-density polyethylene nanocomposites produced in an industrial scale. J Compos Mater 50:3445–3456. https://doi.org/10.1177/0021998315621371
46. Tolinski M)2015(Additives for polyolefins: getting the most out of polypropylene, polyethylene and TPO; William Andrew, second edition
47. Peacock A (2000) Handbook of polyethylene: structures: properties and applications. CRC Press, Florida
48. Maier C, Calafut T. (1998) Polypropylene: the definitive user's guide and databook; William Andrew
49. Erbetta CD, Manoel GF, Oliveira AP, Silvae ME, Freitas RF, Sousa RG (2014) Rheological and thermal behavior of high-density polyethylene (HDPE) at different temperatures. Mater Sci Appl 5:923–931
50. Afzali K, Keshavarzian A, Rashedi R (2014) Effect of change in phosphite antioxidant additives on degradation behavior of linear low density polyethylene film grade. The 8th international Chemical Engineering Congress and Exhibition.
51. Hirotsu T, Ketelaars AA, Nakayama K (2000) Biodegradation of poly(Ɛ-caprolactone)–polycarbonate blend sheets. Polym Degrad Stab 68:311–316. https://doi.org/10.1016/S0141-3910(99)00156-1
52. Arutchelvi J, Sudhakar M, Arkatkar A, Doble M, Bhaduri S, Uppara PV (2008) Biodegradation of polyethylene and polypropylene. Indian J Biotechnol 7:9–22
53. Abdel-Hakim A, Mourad RM (2020) Mechanical, water uptake properties and biodegradability of polystyrene-coated sisal fiber-reinforced high-density polyethylene. Polym Compos 41:1435–1446. https://doi.org/10.1002/pc.25467
54. Chiellini E, Corti A, D'Antone S (2007) Oxo-biodegradable full carbon backbone polymers e biodegradation behaviour of thermally oxidized polyethylene in an aqueous medium. Polym Degrad Stab 92:1378–1383. https://doi.org/10.1016/j.polymdegradstab.2007.03.007
55. Scalenghe R (2018) Resource or waste? A perspective of plastics degradation in soil with a focus on end-of-life options. Heliyon 4:e00941
56. Campos AD, Marconato JC, Martins-Franchetti SM (2012) The influence of soil and landfill leachate microorganisms in the degradation of PVC/PCL films cast from DMF. Polímeros 22:220–227. https://doi.org/10.1590/S0104-14282012005000029
57. Liu W, Wang YJ, Sun Z (2003) Effects of polyethylene-grafted maleic anhydride (PE-g-MA) on thermal properties, morphology and tensile properties of low-density polyethylene (LDPE) and corn starch blends. J Appl Polym Sci 88:2904–2911. https://doi.org/10.1002/app.11965
58. Aljabori TMS, Abdellah SF, El-Rafey ME (2020) The influence of adding polycaprolactone and polyethylene grafted maleic anhydride on the mechanical, morphological and biodegradation properties of HDPE. Indian J Nat Sci 10:18104–18109